Biophysical Aspects of Auger Processes, AAPM Symposium Series No. 8 (1992) 121-136
Eds. RW Howell, VR Narra, KSR Sastry, DV Rao

^{123}I: CALCULATION OF THE AUGER ELECTRON SPECTRUM AND ASSESSMENT OF THE STRAND BREAKAGE EFFICIENCY

EKKEHARD POMPLUN

Abteilung Sicherheit und Strahlenschutz,
Forschungszentrum Jülich GmbH, Postfach 1913, D-5170 Jülich,
Germany

ABSTRACT

Auger cascades induced by electron capture in ^{123}I have been simulated by the Monte Carlo technique with special emphasis on the determination of the electron kinetic energies. By using an approach which considers the individual electron population of all electronic shells before and after a transition, errors in the electron energy normally introduced when applying the so-called (Z+1)-approximation are avoided. Thus, the energy of the electrons released in transitions between higher shells were found to be about half the value mentioned in the literature. An average total number of 7.6 electrons (6.4 Auger-, and 1.2 shake-off electrons) has been determined to be emitted per decay, a number which is considerably lower than those reported in similar studies. The efficiency of strand break induction has been assessed to be 0.4 DSB and 1.1 additional SSB per decay of DNA bound ^{123}I. A comparison with the corresponding DSB values of ^{125}I reveals that ^{125}I is 2.5 times more effective than ^{123}I. This is about the same ratio as that determined by Makrigiorgos (1) on the basis of cell killing experiments.

INTRODUCTION

Auger electron emitting nuclides incorporated into sensitive biological structures like DNA have been demonstrated to be of extremely high effectiveness in inducing radiobiological damage (2-5). Furthermore, it has been shown experimentally by Martin and Haseltine (6) and theoretically by Charlton (7) that the initial damage is restricted to the immediate region surrounding the decay site. Although different mechanisms are believed to be involved in the damage process, the electron radiation is expected to be the most important one. To understand the underlying physical and biochemical mechanisms leading to the expression of the biological effects, an accurate description of the radiation source emissions is required.

Since Auger electron emitters decay by a complex process of electronic deexcitation, an evaluation of mean numbers of emitted electrons and their kinetic energies may be sufficient for radiation protection purposes but they are of limited significance for an interpretation of radiation induced biological damage (8). To obtain detailed information about the emitted electrons, a Monte Carlo technique can be used to simulate Auger cascades on the computer. An essential feature of these simulations is the kinetic energy calculation of the electrons released by individual Auger and Coster-Kronig transitions inside the electronic shells of the nuclide.

The first Monte Carlo code simulating an electron capture induced decay and the subsequent electron cascades was written by Charlton and Booz (9) for ^{125}I. In this code the so-called (Z+1)-approximation was used to determine the electron energies. Charge neutralization was considered by filling O-shell vacancies during the cascade process, although, as the authors stated, 'this is difficult to understand physically, since it assumes a very rapid charge transfer'. Applying these two conditions ((Z+1)-approximation and rapid and complete neutralization) results in a broad distribution for the number of electrons emitted (up to more than 40 electrons) with an average number of 21 electrons per decay (9).

It was shown later (10) that the (Z+1)-approximation leads to discrepancies in the total electron energy emitted. As an example, the summation of the kinetic electron energies released after photo-induced Auger cascades in iodine yields, for most deexcitation pathways, more energy than that having been transferred to the nuclide by the incident photon (see Fig. 1). Therefore, the code of Charlton and Booz (9) has been further developed with special emphasis on the calculation of the electron kinetic energies (11). By introducing Dirac-Fock methods that consider the individual

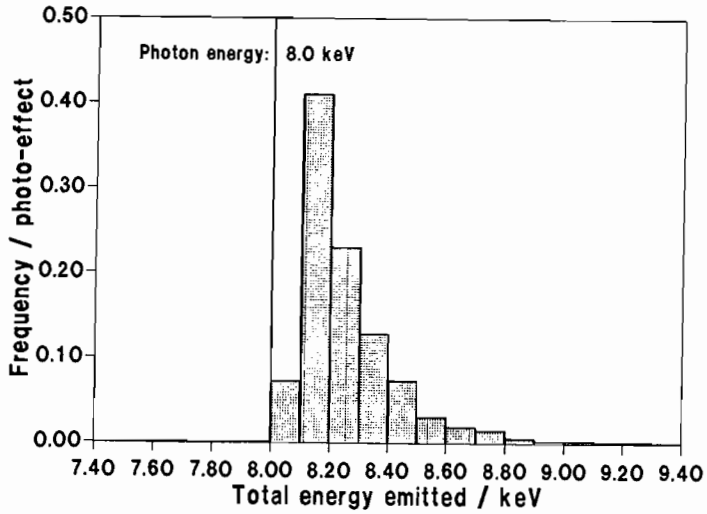

FIG. 1. Energy balance for simulated photon induced (E_{phot} = 8.0 keV) Auger cascades in cold iodine using the (Z+1)-approximation (frequency values are normalized to unity).

electronic configuration of the different shells before and after the Auger transition, an accurate determination of the electron kinetic energy is possible. The emitted energy can be assumed to result from the kinetic energy of the released Auger electrons and from an ionization potential build-up on the daughter atom during the electron cascade. Neutralization of vacancies during the very fast Auger cascade (10^{-16} - 10^{-14} s) is not possible. Vacancies will become neutralized during the comparably long-lived metastable state between two cascades such as the 0.035 MeV state of ^{125}Te (1.6 ns). The electron number distribution calculated for ^{125}I by this approach (11) is much smaller (only up to less than 30 electrons) than the one of Charlton and Booz (9) and the mean number of electrons emitted per ^{125}I decay has been evaluated to be about 13 instead of 21 (see above). This number approximates the number calculated by Charlton and Booz (9) and by Humm (16) for an isolated ^{125}I atom. Detailed comparison of both codes by tracing single cascades showed that the kinetic energies evaluated by the (Z+1)-approximation will be considerably overestimated, particularly for those electrons from higher shells that are mainly emitted when the shells already have been significantly depleted.

In further investigations with ^{125}I, track structures of the emitted Auger electrons generated by the code of Paretzke (12) were superimposed on DNA volume models of different geometrical resolutions (13,14). Again the locally restricted effectiveness of the Auger electrons could be demonstrated as well as the fact that the Auger electrons with a kinetic energy of less than 500 eV play the dominant role in the induction of single- and double strand breaks (14). Mostly originating from higher shell transitions, these electrons are the ones which are most strongly affected by an uncertain energy determination.

Until now the technique of energy calculation by the Dirac-Fock method has been applied to ^{125}I only. Another possibly useful nuclide in radiation biology is ^{123}I. This isotope has a 13.2 h half-life, compared to 60.1 d for ^{125}I, and is routinely used as an imaging isotope in nuclear medicine. Its decay scheme (see Fig. 2) is much more complex than that of ^{125}I insofar as the

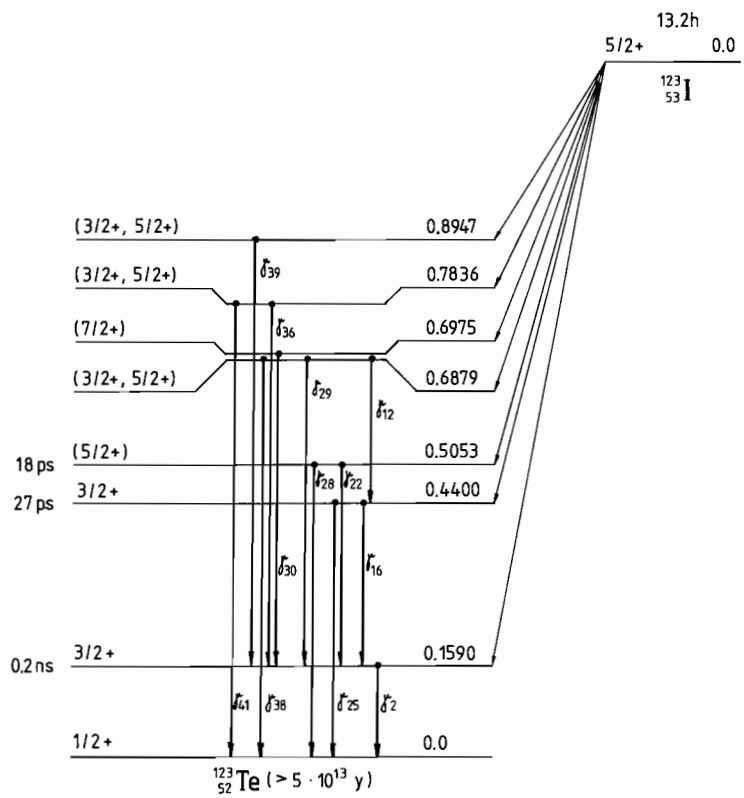

FIG. 2. Decay scheme of ^{123}I.

EC process (100%) may lead to different excited ^{123}Te states depending on the branching ratios (see legend of Table I). Most frequently (> 97%) the decay goes to the 159 keV level and subsequently, either by γ emission (84%) or by internal conversion (IC), to the ground state of ^{123}Te. Since only 16% of the ^{123}I decays result in internal conversion, only this percentage of decays give rise to two Auger cascades compared to 93% for ^{125}I. Recent radiobiological measurements performed with ^{123}I refer to the end point of cell survival (1) and reveal that 2.2 ± 0.3 times more ^{123}I decays are necessary to induce the same degree of cell death as with ^{125}I, whereas the mean lethal dose (D_{37}) to the nucleus is about the same for both nuclides. Because their Auger electron cascades are identical but the numbers of cascades are different, a comparison of the biological efficiencies of these nuclides will be of interest since - if the electron irradiation is mainly responsible for the biological effect - it should be possible to compare the different biological effectiveness in relation to the differences in the electron tracks and their energy deposition in the DNA.

TABLE I

Electron Capture and Internal Conversion Probabilities for the 0.159 MeV Level of ^{123}Te.

Shell	EC	IC
K	0.797	0.135
L_1	0.104	0.016
L_2	0.003	0.0011
L_3	0.007	0.0004
M_1	0.022	0.0035
M_2	0.001	0.0
M_3	0.038	0.0
M_4	0.0	0.0
M_5	0.0	0.0
N_1	0.005	0.0008
N_2	0.0	
N_3	0.0	

For other energy levels the following EC values have been used: 0.44 MeV: 0.004 (K shell), 0.506 MeV: 0.003 (K shell), 0.6975 MeV: 0.014 (K shell) and 0.002 (L_1 shell). IC values for other levels than 0.159 MeV were neglected. The EC data were taken from Humm (16), the IC data from ICRP (17).

In this work the number distribution of Auger electrons emitted by ^{123}I decays will be calculated and compared with results from the literature obtained by application of the (Z+1)-approximation. The presentation of the mean ^{123}I Auger electron spectrum together with the one of ^{125}I illustrates the characteristic differences between these two radiation sources. The effectiveness of strand break induction by DNA-incorporated ^{123}I will be assessed by superimposing electron track structures on a DNA target model of atomic scale resolution (14).

METHODS

A detailed description of the applied Monte Carlo program for the simulation of Auger cascades is given by Pomplun et al. (11) for the case of ^{125}I decay. Therefore, only a very brief description of the characteristics of this code and the necessary alterations for ^{123}I will be summarized. The code traces the different steps of the nuclide decay starting with the selection of the ^{123}Te energy level resulting from the EC transition and the shell from which the electron will be captured (in about 80% from the K shell; see Table I). Individual Auger- and Coster-Kronig transitions are chosen by the weighted probability distribution of all transitions energetically allowed in the single ionized atom. Each transition is tested by a special algorithm which calculates quite accurately by a relativistic Dirac-Fock approach (15) the total energy of the nuclide with the actual individual electron configuration at any step during the cascade. An Auger transition suggested by the random numbers will be checked with regard to the energy difference between the configurations before and after the transition. If a positive amount is evaluated it will be assigned to the kinetic energy of the emitted Auger electron. In case of a negative energy value the transition will be considered as energetically not possible at that stage of the cascade. The probabilities of the remaining transitions will be renormalized. Furthermore, whenever a transition is selected, the possibility of shake-off electron emission is tested and - when outer shells are involved in the transition - double Auger processes are also taken into account. The cascade comes to an end if no more transitions are energetically possible. The sources for the required input data are given in Ref. (9) and (11). To get sufficient statistics the calculations reported here have been performed for 10000 ^{123}I decays.

The kinetic energies of the individual Auger and conversion electrons for each decay provided by the cascade program were recorded as input data for the MOCA8 code of Paretzke (12). This code generates track structures of electrons in water vapor, a medium which poses some limitations to the comparability with real biological tissue. Those limitations are discussed in

detail by Charlton and Humm (13) and by Pomplun (14). The application of water vapor cross-sections in this work, therefore, means that the sizes of the energy transfer events and their positions relative to the site of decay can be seen as an approximation only.

The employed DNA target model (Fig. 3) is characterized by its high geometrical resolution which became possible by using the coordinates of the single atoms of the double helix molecule (18,19). Due to this atomic scale, a distinction has been made between the direct and the indirect hit mode of radiation action - according to the definition given by Dertinger and Jung (20) - when the interaction of electrons with the DNA were simulated. After shifting the starting point of the electrons to the assumed position of the incorporated iodine (the methyl group of a thymine base), then, for each energy transfer event from the electron tracks, the program DNAMOD (14) looks for the nearest atom, and the event is considered to be a direct hit if its position lies within the van der Waals radius of that atom. If the event's position is outside of the atomic volumes but inside a virtual straight cylinder - representing a DNA segment including the structural water molecules - then an indirect hit is assumed. The program registers these events separately from those recognized as direct events.

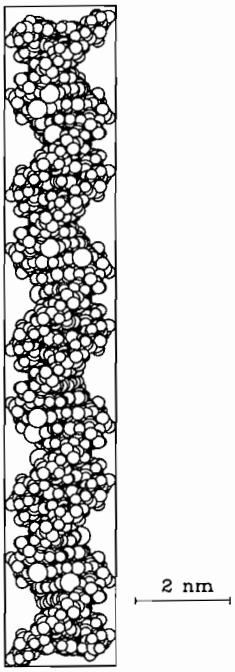

FIG. 3. DNA target model; the straight cylinder indicates the total DNA segment including structural water molecules located preferably in the grooves.

Different energy threshold values have been applied for the assessment of strand break induction by direct and indirect hits. For the direct hit mode, an energy deposition of $E \geq 10$ eV inside the phosphate/sugar chain was assumed to be necessary to induce a SSB due to the fact that ionization potentials of biomolecules are below this value (21). According to Chatterjee and Magee (22) a radical pair requires an energy of $E \geq 17$ eV in the surrounding water to be created; this value has been taken as the threshold for indirect hits. In a very simple approximation a strand break by radical attack is assumed if the nearest atom of the DNA molecule to an indirect hit position belongs to the phosphate or sugar group. A DSB will be recorded if there are two SSB on complementary strands less than 20 base pairs apart from each other (for details see Ref. (14)). Whereas SSB can be induced by direct or indirect hits, compound hits have to be considered for DSB, *i.e.* one strand is broken by a direct, the other by an indirect hit. This implies that the total number of DSB might be greater than the sum of DSB induced by direct or indirect hits only. Other mechanisms of strand breaks, *e.g.* via base damage, have been neglected here.

RESULTS AND DISCUSSION

The calculated numbers of the emitted electrons are given in Table II (mean values per decay) and in Fig. 4 (frequency distribution). Following the approach developed by Pomplun *et al.* (11) the term 'condensed phase', as it is used in this work, implies boundary conditions in the application of the Monte Carlo code different from those used by Humm (16) and by Sastry and Rao (23) (see Introduction). Because of the assumptions made in Ref. (16) and (23) for the charge transfer velocity, the values reported in these investigations can be seen as an upper limit. However, a rough comparison might be reasonable between the 'isolated atom' case in Ref. (16) yielding 8.9 electrons and the 'condensed phase' situation of this work (one cascade only in 84% of the decays and also no neutralization during the cascade) yielding 6.4 electrons. The additional 1.2 shake-off electrons found here result from a different mechanism which was not taken into account by Humm (16). Thus, the difference in the energy determination leads to a difference in the mean value of emitted Auger electrons of about 2.5 per decay. A similar difference in the mean number of emitted electrons can be found for ^{125}I. For the case of a completely isolated atom (even during the metastable state with a half-life of 1.6 ns no neutralization has been assumed) 13.2 electrons have been calculated with the (Z+1)-approximation but only 10.1 electrons using the Dirac-Fock approach (11). The present frequency distribution for the number of emitted electrons (Fig. 4) compared with that of Humm (16) covers the same range but the maximum is shifted to a smaller value.

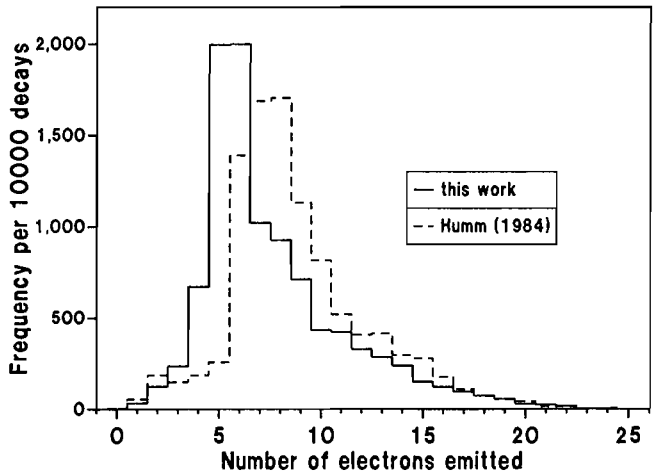

FIG. 4. Distribution of the number of emitted electrons, comparison with results obtained by (Z+1)-approximation (16).

TABLE II

Electron Yield per ^{123}I decay: Comparison with (Z+1)-Approximation

Radiation	This work	Humm (16)		Sastry and Rao (23)
	Cond. Phase	Isol. Atom	Cond. Phase	Cond. Phase
Auger Coster-Kronig Electrons	6.4	8.9	12.3	11
Shake-off Electrons	1.2	-	-	-

The term 'condensed phase' in this work means that charge transfer took place only during the metastable states of ^{123}Te whereas in the work of Humm (16) and Sastry & Rao (23) a permanent neutralization of O shells is assumed.

The mean values for frequencies and energies of the emitted radiation per ^{123}I decay are listed in Table III. These values are compared with the corresponding ones determined by ICRP (17) on the basis of a (Z+1)-approximation. Whereas the energy differences for Auger electrons resulting from transitions to the K shell are less than 1%, and those to the L shells are less than 5%, for transitions to higher shells the Auger electron kinetic energy is about 55% of the corresponding ICRP value (MXY-transitions). Coster-Kronig electrons as well as N shell Auger electrons and shake-off electrons are not mentioned by ICRP (17). The mean ionization potential at the end of the ^{123}I Auger cascade has been evaluated here to be 0.577 keV, as expected, about one half of the corresponding value (1.07 keV) for ^{125}I (11).

A comparison of the energy spectra between ^{123}I and ^{125}I (Fig. 5) shows that - as expected - all ^{123}I Auger- and Coster-Kronig electrons have identical energy values but reduced frequencies. The qualitative differences between these two spectra result from the conversion electrons which lie for ^{123}I in the energy range above 100 keV with frequencies comparable to most Auger electrons. In contrast, the conversion electron from the K shell represents the most prominent line in the ^{125}I spectrum, appearing in nearly each (83%) decay.

The results for the strand break efficiency are presented in Table IV. The total, as well as the corrected, numbers of SSB are given for both mechanisms (direct and indirect) and for all hits separately. Due to compound hits (see METHODS) the total number of DSB is greater than the sum of DSB induced by direct and indirect hits only. Therefore, the corrected numbers for 'all hit' SSB are not necessarily the sum of the corresponding direct and indirect hit values (see also Ref. (14)). The number of total SSB induced by ^{123}I yields nearly 2 per decay, just half the number of ^{125}I induced breaks. This value seems to be reasonable due to the fact of having, in most decays, one electron cascade in the tellurium daughter atom instead of two like in the great majority of ^{125}I decays. But for DSB the situation is different. About 40% of the ^{123}I decays produce a DSB whereas the corresponding efficiency of ^{125}I is 100%, *i.e.* on average each ^{125}I decay induces one DSB. To assess the influence of the conversion electrons which are responsible for the qualitative difference in the electron spectra of ^{123}I and ^{125}I, separate calculations (data not shown here) have been performed for ^{125}I electron spectra without the conversion electrons (which appears in 93% of all decays). The contribution to strand break induction by these electrons was found to be negligibly small (less than 3% of all SSB).

TABLE III. ^{123}I Radiation Spectrum

Radiation	Frequency per decay		Mean energy (keV)	
	this work	ICRP (17)	this work	ICRP (17)
γ_2	0.8391	0.828	159.0	159.0
γ_{12}	0.0004	0.0007	248.0	248.0
γ_{16}	0.0011	0.0008	281.0	281.0
γ_{22}	0.0009	0.0013	346.3	346.3
γ_{25}	0.0033	0.0043	440.0	440.0
γ_{28}	0.0020	0.0031	505.3	505.3
γ_{29}	0.0115	0.0138	529.0	529.0
γ_{30}	0.0038	0.0038	538.5	538.5
γ_{36}	0.0003	0.0008	624.6	624.6
γ_{38}	0.0002	0.0003	687.9	687.9
γ_{39}	0.0006	0.0006	735.8	735.8
γ_{41}	0.0003	0.0006	783.6	783.6
ce-K	0.1341	0.135	127.123	127.2
ce-L_1	0.0151	0.016	154.028	154.0
ce-L_2	0.0008	0.0011	154.371	154.4
ce-L_3	0.0004	0.0004	154.647	154.6
ce-M_1	0.0037	0.0035	157.973	158.2
ce-N_1	0.0010	0.0008	158.811	159.0
$K_{\alpha 1}$	0.4452	0.458	27.444	27.47
$K_{\alpha 2}$	0.2466	0.246	27.214	27.20
$K_{\beta 1}$	0.0814	0.0866	30.984	31.0
$K_{\beta 2}$	0.0222	0.0266	31.688	31.71
$K_{\beta 3}$	0.0415	0.0446	30.935	30.94
$K_{\beta 5}$	0.0008	-	31.235	-
$L_{X\text{-ray}}$	0.0837	-	3.935	-
AUG KLL	0.0751	0.0815	22.499	22.54
AUG KLX	0.0367	0.0369	26.418	26.35
AUG KXY	0.0029	0.0049	30.179	30.13
C-K LLX	0.1432	-	0.279	-
AUG LMM	0.7187	0.606	3.018	3.080
AUG LMX	0.2003	0.311	3.650	3.849
AUG LXY	0.0116	0.044	4.265	4.380
C-K MMX	0.8587	-	0.095	-
AUG MXY	1.9473	1.80	0.383	0.699
AUG NXY	2.2614	-	0.031	-

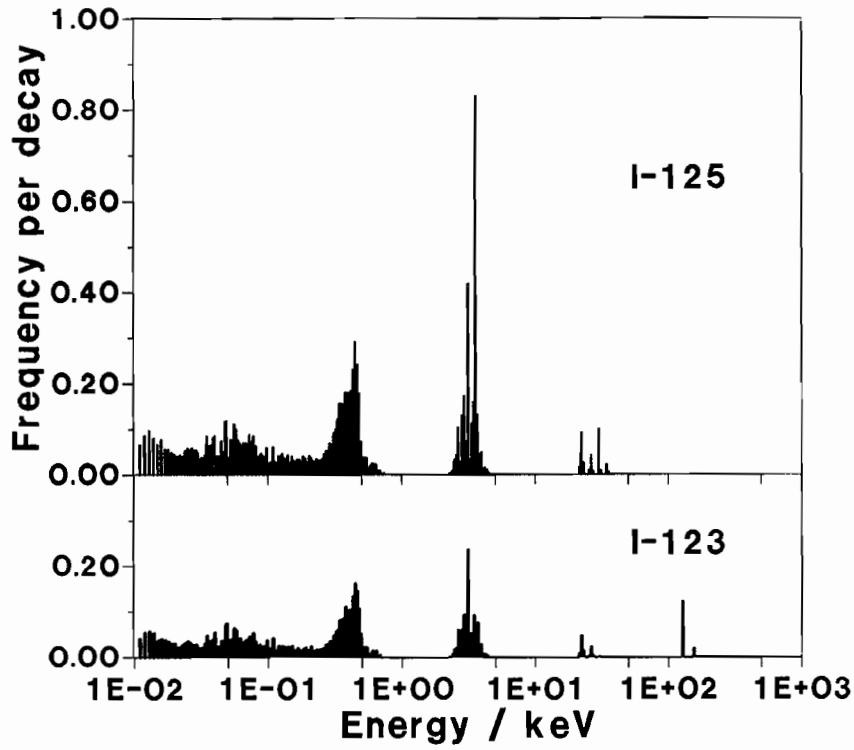

FIG. 5. Mean electron spectra of ^{123}I and ^{125}I.

A direct comparison with experimental results is not possible due to the lack of data for strand break induction. However, since there is strong indication that cell death is directly related to the number of DSB (24-26) it seems justified to compare the ratio between the numbers of ^{125}I (14) and ^{123}I (this work) induced DSB with the ratio of 2.2 ± 0.3 obtained experimentally by Makrigiorgos *et al.* (1) for the total number of ^{123}I decays versus ^{125}I decays to find the same level of cell survival. The calculated values for DSB induction per decay by ^{125}I, 1.0, and by ^{123}I, 0.4, (see Table IV) result in a corresponding ratio of 2.5 which is inside the uncertainty range of the experimentally found value. Strand break induction, as it is considered here, is due to electron radiation only; *i.e.* if the underlying assumptions are correct, then the Auger electrons are responsible for the biological effects discussed here. This is also supported by the finding of Makrigiorgos *et al.* (1) that Auger electron irradiation is the predominant reason for the observed biological toxicity.

Under these implications the ionization potential built up during the Auger cascade on the Te-daughter atom and the subsequent charge transfer processes would be of minor significance.

TABLE IV
Number of DNA Strand Breaks per Decay Induced by Direct and Indirect Hits

	Direct Hits		Indirect Hits		All Hits	
	^{123}I	^{125}I	^{123}I	^{125}I	^{123}I	^{125}I
SSB (tot.)	1.1	1.9	0.8	2.1	1.9	4.0
SSB (corr.)	0.7	1.1	0.6	1.2	1.1	2.0
DSB	0.2	0.4	0.1	0.5	0.4	1.0

The ^{125}I data had been slightly changed against the values reported in Ref. (14) because of a revision to eliminate a minor program error. In the last column ('all hits') no distinction was made between the hit modes, so that for total SSB the values are just the sum of the breaks from direct and indirect hits, whereas in case of DSB compound hits also contributed to the figure.

CONCLUSIONS

The electron capture induced decay of ^{123}I has been simulated by a Monte Carlo technique to calculate the electron emission spectrum and to assess the biological efficiency when this nuclide is incorporated into the DNA molecule. Since the Auger electrons with $E \leq 500$ eV are the main contributors to strand break induction subsequent to electron capture decay, the determination of the electron kinetic energies is of particular interest. By application of an approach using Dirac-Fock methods it has been possible to take into account the influence of complex electron configurations on the binding energies of those electrons involved in the individual Auger transitions. The calculations performed here reveal a mean total number of 7.6 emitted electrons per decay (6.4 Auger and Coster-Kronig electrons and 1.2 additional shake-off electrons). This number is about 30% less than that obtained by Humm (16) for a comparable situation with the (Z+1)-approximation although the broadness of the distribution is about the same. The electron kinetic energies are smaller than those previously reported *e.g.* by ICRP (17), in particular those in the energy range below 500 eV. Specifically, for the MXY transition electrons (Table III), the kinetic energies were reduced by 45% compared with the ICRP energies.

The effectiveness of DNA-incorporated ^{123}I to induce SSB by electron irradiation has been found to be about 0.5 of the corresponding ^{125}I value due to the reduced intensity of the Auger electron spectrum by about one half according to its decay characteristics. If one compares the evaluated numbers of DSB produced by these two nuclides, ^{125}I appears to be 2.5 times more effective than ^{123}I. Nearly the same relation (2.2 ± 0.3) was found by Makrigiorgos *et al.* (1) for cell survival in an experimental investigation. Since here in this work only electron interaction with DNA has been considered, the similarity of both values could be an indication that neutralization processes do not significantly contribute to the induction of strand breaks. However, to further elucidate the different possible mechanisms of radiation action, experimental measurements of strand break induction by ^{123}I would be most desirable.

ACKNOWLEDGMENTS

The author thanks Dr. H.G. Paretzke, GSF Neuherberg, for use of the MOCA8 code for the generation of track structures.

REFERENCES

1. G.M. MAKRIGIORGOS, A.I. KASSIS, J. BARANOWSKA-KORTYLEWICZ, K.D. McELVANY, M.J. WELCH, K.S.R. SASTRY, and S.J. ADELSTEIN, Radiotoxicity of 5-[^{123}I]Iodo-2'-deoxyuridine in V79 cells: A comparison with 5-[^{125}I]Iodo-2'-deoxyuridine. *Radiat. Res.* **118**, 532-544 (1989).
2. L.E. FEINENDEGEN, H.H. ERTL, V.P. BOND, Biological toxicity associated with the Auger effect. *Proc. Symposium Biological Aspects of Radiation Quality*, p. 419-429, International Atomic Energy Agency, Vienna, SM-145-22, 1971.
3. R. ROOTS, L.E. FEINENDEGEN, and V.P. BOND, Comparative radiotoxicity of ^{3}H-IUdR and ^{125}IUdR after incorporation into DNA of cultured mammalian cells. In *Proc. Third Symposium on Microdosimetry*, pp. 371-388, Report EUR 4810, (H.G. Ebert, Ed), Commission of the European Communities, Luxembourg, 1971.
4. K.G. HOFER, C.R. HARRIS and J.M. SMITH, Radiotoxicity of intracellular ^{67}Ga and ^{125}I and ^{3}H. Nuclear versus cytoplasmic radiation effects in murine L1210 leukemia. *Int. J. Radiat. Biol.* **28**, 225-241 (1975).
5. A.I. KASSIS, F. FAYAD, B.M. KINSEY, K.S.R. SASTRY, and S.J. ADELSTEIN, Radiotoxicity of an ^{125}I-labelled DNA intercalator in mammalian cells. *Radiat. Res.* **118**, 283-294 (1989).
6. R.F. MARTIN and W.A. HASELTINE, Range of radiochemical damage to DNA with decay of iodine-125. *Science* **213**, 896-898 (1981).
7. D.E. CHARLTON, The range of high-LET effects from ^{125}I decays. *Radiat. Res.* **107**, 163-171 (1986).
8. D.E. CHARLTON, Comments on strand breaks calculated from average doses to the DNA from incorporated isotopes. *Radiat. Res.* **114**, 192-197 (1988).
9. D.E. CHARLTON and J. BOOZ, A Monte Carlo treatment of the decay of ^{125}I. *Radiat. Res.* **87**, 10-23 (1981).

10. E. POMPLUN, Mikrodosimetrische Berechnung der Energiedeposition und des Dosisgrenzwertes nach Zerfall von Radionukliden in biologischen Systemen. *Ph.D. Dissertation*, Universität Düsseldorf, 1987.
11. E. POMPLUN, J. BOOZ, and D.E. CHARLTON, A Monte Carlo simulation of Auger cascades. *Radiat. Res.* **111**, 533-552 (1987).
12. H.G. PARETZKE, Radiation track structure theory. In *Kinetics of Nonhomogeneous Processes*, (G.R. Freeman, Ed.) Wiley, New York, pp. 89-170, 1987.
13. D.E. CHARLTON and J.L. HUMM, A method of calculating initial DNA strand breakage following the decay of incorporated ^{125}I. *Int. J. Radiat. Biol.* **53**, 353-365 (1988).
14. E. POMPLUN, A new DNA target model for track structure calculations and its first application to I-125 Auger electrons. *Int. J. Radiat. Biol.* **59**, 625-642 (1991).
15. J.P. DESCLAUX, A multiconfiguration relativistic Dirac-Fock program. *Comput. Phys. Commun.* **9**, 31-45 (1975).
16. J.L. HUMM, The analysis of Auger electrons released following the decay of radioisotopes and photoelectric interactions and their contribution to energy deposition. *Bericht der Kernforschungsanlage Jülich*, Jül-1932, 1984.
17. ICRP, *Radionuclide Transformations*, Publication 38, International Commission on Radiation Protection and Standards, Pergamon Press, Oxford.
18. S. ARNOTT and D.W.L. HUKINS, Refinement of the structure of B-DNA and implications for the analysis of X-ray diffraction data from fibers of biopolymers. *J. Mol. Biol.* **81**, 93-105 (1973).
19. R. CHANDRASEKARAN and S. ARNOTT, The structures of DNA and RNA helices in oriented fibers. *Landolt-Börnstein, New Series* VII, 1b, Springer-Verlag, Berlin, 1989.
20. H. DERTINGER and H. JUNG, *Molekulare Strahlenbiologie*, Springer Verlag Berlin, 1969.
21. M. INOKUTI, Atomic processes pertinent to radiation physics. *Electronic and Atomic Collisions*, (N. Oda and K. Takayanagi, Eds.), North-Holland Publishing Company, Amsterdam-London, pp. 31-45, 1980.
22. A. CHATTERJEE and J.L. MAGEE, Theoretical investigation of the production of strand breaks in DNA by water radicals. *Radiat. Prot. Dosim.* **13**, 137-140 (1985).
23. K.S.R. SASTRY and D.V. RAO, Dosimetry of low energy electrons. In *Physics of nuclear medicine: Recent advances.* (D.V. RAO, R. CHANDRA, and M.C. GRAHAM, Eds.) American Association of Physicists in Medicine, Medical Physics Monograph No 10, American Institute of Physics, New York, pp. 169-208, 1984.
24. I.R. RADFORD, The level of induced DNA double-strand breakage correlates with cell killing after X irradiation. *Int. J. Radiat. Biol.* **48**, 45-54 (1985).
25. P.E. BRYANT, Enzymatic restriction of mammalian cell DNA: Evidence for double strand breaks as potentially lethal lesions. *Int. J. Radiat. Biol.* **48**, 55-60 (1985).
26. M. FRANKENBERG-SCHWAGER, Induction, repair and biological relevance of radiation induced DNA lesions in eukaryotic cells. *Radiat. Environ. Biophys.* **29**, 273-292 (1990).

DISCUSSION

Kassis, A. I. What are the assumptions of > 10 keV and > 17 keV needed for direct and indirect effects based on?

Pomplun, E. They were taken from the literature.

Halpern, A. What do you mean when you say indirect effects?

Pomplun, E. Effects mediated by vehicles, *e.g.* radicals.

Halpern, A. Water radicals?

Pomplun, E. Yes.

Halpern, A. DNA structural water is not vapor. It changes the physical properties of DNA (*e.g.* its conductivity).

Pomplun, E. The calculations presented here have been performed for a DNA model. It is obvious that such a model has its restrictions. Of course, this model - compared with real DNA - is a very simple one because it neglects a number of physical, chemical, and biological DNA properties (*e.g.* the conductivity). These properties can be incorporated into the model step by step as far as appropriate data for the different properties are available. Furthermore, in the special case of this paper, although the calculated absolute values of strand breaks might be of less reliability due to the incomplete DNA model, the relation between ^{123}I and ^{125}I induced strand breaks gives a reasonable value.